

A micromachined nanoindentation force sensor

Alexandra Nafari^{a,c,*}, Andrey Danilov^{c,d}, Henrik Rödjegård^e,
Peter Enoksson^a, Håkan Olin^b

^a Solid State Electronics Laboratory, Department of Microtechnology and Nanoscience, Chalmers University of Technology, SE-412 96 Kemivägen 9, Göteborg, Sweden

^b Department of Engineering, Physics, and Mathematics, Mid Sweden University, SE-851 70 Sundsvall, Sweden

^c Nanofactory Instruments AB, Walleriusgatan 2, SE-412 58 Göteborg, Sweden

^d Department of Microtechnology and Nanoscience, Chalmers University of Technology, SE-412 96 Göteborg, Sweden

^e Imego AB, Arvid Hedvalls backe 4, SE-411 33 Göteborg, Sweden

Received 13 September 2004; received in revised form 21 March 2005; accepted 31 March 2005

Available online 8 June 2005

Abstract

A capacitive force sensor for in situ nanoindentation experiments in TEM has been designed, manufactured and evaluated. The confined space of the TEM specimen holder restricts the size of the fabricated sensor to $2\text{ mm} \times 1.5\text{ mm} \times 2\text{ mm}$ to allow mounting. A unique feature of the sensor is an integrated fixture for interchangeable tips, e.g. diamond tips. The sensor is fabricated in silicon anodically bonded to glass and the device is formed by DRIE. To improve the control of spring thickness and circumvent problems during fabrication a SOI wafer and slightly altered design was used in conjunction to an improved process, which resulted in a yield near 100%. The sensor is characterized by a force application using a piezoelectric positioning system, an electrostatic evaluation and a resonance frequency test using a scanning laser doppler vibrometer. The capacitance is measured with an off-chip read-out circuit. The resonance frequency test yielded a spring constant of 750 N/m , which results in a sensitivity of $0.27\text{ pF}/0.1\text{ }\mu\text{N}$ for small deflections. The evaluation shows that the force sensor is suitable for in situ nanoindentation for measurements in the range of $0\text{--}100\text{ }\mu\text{N}$.

© 2005 Elsevier B.V. All rights reserved.

Keywords: Force sensor; Capacitive detection; Nanoindentation; Microfabrication; Transmission electron microscope; Interchangeable tip

1. Introduction

Nanoindentation is used for the study of mechanical properties of materials on the nanoscale. The technique utilizes an actuator to press a sharp diamond tip a few nanometer into the sample while measuring the applied force, typically giving information about the hardness or elastic modulus of the material in the sub-micron regime [1]. The data obtained by the nanoindentation method have been limited to the load–displacement data and, by the lack of direct observation of the induced plastic deformation, to ex situ studies of the analysis of the indentation mark. Recently, however, an extension of the nanoindentation method has

been demonstrated, using a transmission electron microscope (TEM) for in situ imaging of the entire indentation process [2–4], giving new opportunities for material characterization. For example, the in situ nanoindentation method has been used for studies of grain boundary motion in polycrystalline Al films [5], room temperature plasticity in silicon [6] or grain boundary-mediated plasticity in nanocrystalline nickel [7].

This kind of in situ nanoindenter instrument belongs to a new family of probe instruments placed inside the millimeter sized pole gap of the TEM, such as the scanning tunneling microscope combined with a TEM [8,9]. To take full advantage of the new TEM-nanoindentation method, a proper force sensor is needed, which was only used in an indirect way in [2–4]. Here, we report on such a force sensor fabricated by micromachining methods.

* Corresponding author. Tel.: +46 31 772 1866; fax: +46 31 772 3622.
E-mail address: alexandra.nafari@mc2.chalmers.se (A. Nafari).

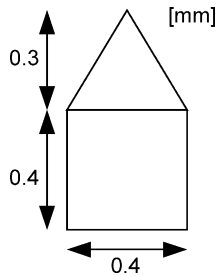


Fig. 1. Geometry and dimension of the nanoindenter tip, the lower part is a cylinder and the upper has a conical part.

2. Sensor requirements

The confined space of the TEM specimen holder restricts the dimensions of the sensor to $2\text{ mm} \times 2\text{ mm} \times 1.7\text{ mm}$. The sensor will also have an integrated fixture for a tip as in see Fig. 1. This is needed to enable a large freedom in the choice of tip configuration and tip materials. Diamond is usually the preferred tip material, but it can for research and economic reasons be advantageous to choose other tip materials. The maximum load specified for the nanoindentation is 10 mN and the working load range is $0\text{--}0.1\text{ mN}$, with a resolution of $0.1\text{ }\mu\text{N}$ [1]. In addition, it is preferred to have multiple directions sensing to give a better overview of the sample.

To realize these requirements a capacitive read-out was chosen. Other read-out methods such as piezoresistive and piezoelectric were also considered but excluded due to manufacturing and consistency problems.

3. Sensor description and fabrication

The force sensor consists of a silicon part acting as top electrode in a capacitive coupling and deposited aluminium on a glass part as lower electrode, see Fig. 2. Glass is chosen for anodic bonding and its high dielectric property. The integrated fixture in the silicon part for the interchangeable tip is relatively large and limits the space for a weak membrane. Therefore, the fixture is suspended with eight identical springs as seen in Fig. 2. This yields the required sensitivity. The silicon plate is connected through a press contact. The press contact consists of two parts, one part is deposited aluminium on the top-side of the glass and second part is the frame of the silicon structure. During anodic bonding, these two parts are pressed tightly in contact constituting the press contact. A possibility to measure the force direction is incorporated in the electrode design. To do this, the lower electrode

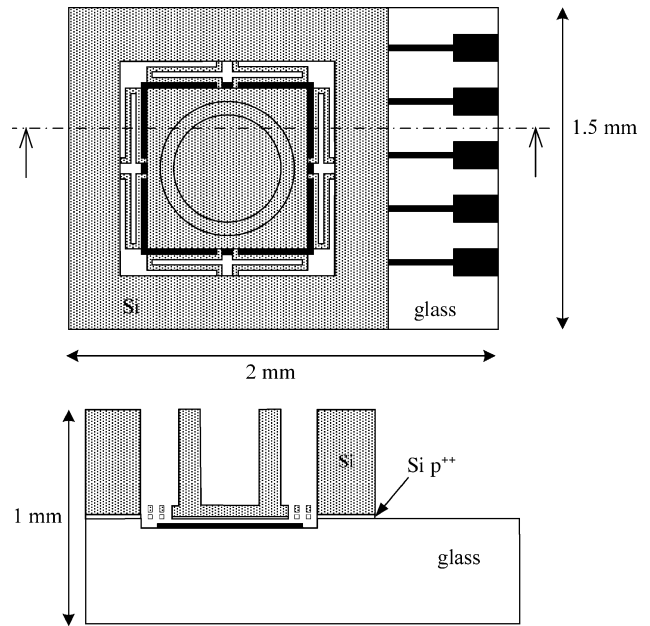


Fig. 2. The capacitive force sensor design.

is divided in four parts in some of the manufactured sensors. The relative capacitance change between the electrode parts gives a measure of the force direction.

The theoretical sensitivity was simulated in FEMLAB using a simplified model. It is assumed that the springs are suspended to a stiff body. This is a reasonable assumption since the fixture and the tip leave almost no room for a membrane. The modelled spring is fixed at one end and constraint in x and y direction at the other end where the force is applied. Different dimensions were simulated. The results are calculated assuming an electrode gap of $1.8\text{ }\mu\text{m}$. The calculations are presented in Table 1.

Choosing a spring thickness of $20\text{ }\mu\text{m}$ yields a theoretical sensitivity of $0.16\text{ fF}/0.1\text{ }\mu\text{N}$ and a spring constant of 1042 for the system. This resolution is measurable with existing read-out chips [10].

3.1. Fabrication

The basic processing steps are shown schematically in Fig. 3. The deep reactive ion etching (DRIE) that forms the fixture and releases the springs is a critical step, Fig. 3(c), where the wafer is etched about $500\text{ }\mu\text{m}$, with a ratio of 1:5. Oxide is grown and patterned to later be combined with resist and used as mask during the DRIE-etch, see Fig. 3(a). The lower part of the silicon is p^{++} doped to form an

Table 1
Simulation results when applying $0.1\text{ }\mu\text{N}$ on a unloaded spring

Spring thickness (μm)	Deflection (m)	Capacitance change (fF)	Spring constant (N/m)
25	$5.32\text{e} - 11$	0.092	1880
20	$9.59\text{e} - 11$	0.16	1042
15	$2.08\text{e} - 10$	0.36	480

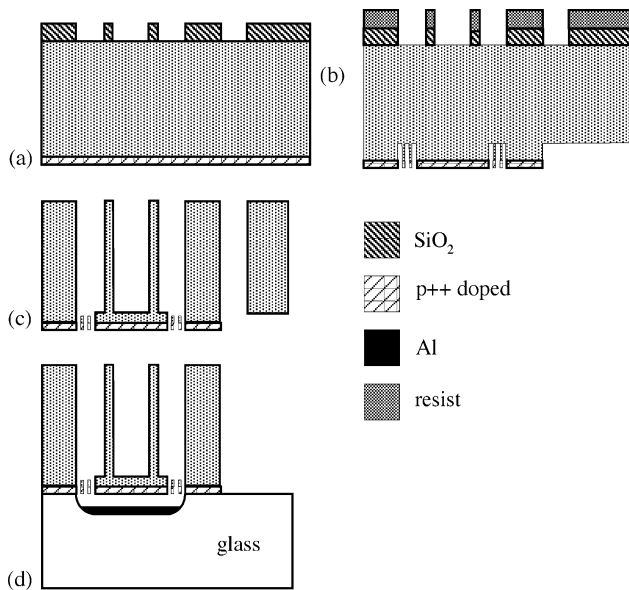


Fig. 3. Schematic of the basic fabrication steps: (a) oxide mask and p++ doping, (b) enhanced oxide mask and etched spring shaping, (c) deep dry etch of the fixture and (d) final anodic bonding.

ohmical contact between the aluminium contact deposited on the glass and the silicon. The spring structure is etched in the lower part with resist as mask, Fig. 3(b). Cavities are etched in the glass and aluminium electrodes deposited. When the glass wafer and the silicon wafer are processed they are anodically bonded together, Fig. 3(d). The anodic bonding was performed with ± 500 – 700 V and 400 °C. To avoid unwanted bonding of the moveable parts, all the electrodes are connected together and also through the press contact connected to the silicon structure, Fig. 4. Thus, the aluminium will be at the same potential as the silicon, resulting in no attractive electrostatic forces during the anodic bonding. This connection of the electrode is removed in the final dicing.

The press contact used to connect the silicon part caused problems during the bonding. It was 1 μm thick to start with and the bonding was not sufficient, Fig. 4(a). The aluminium was thinned to 0.45 μm , which solved this problem, Fig. 4(b).

There were several problems with this process plan resulting in a low yield, where the DRIE-etch was the most critical step. The time stop used, gave little control over the dimension of the springs and many of the fixtures were etched off

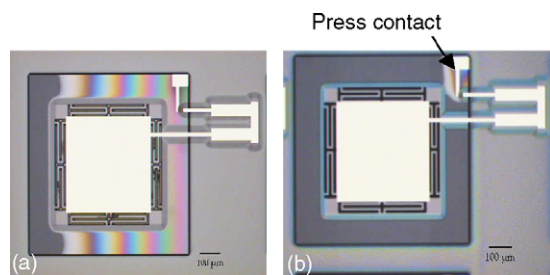


Fig. 4. Anodic bonding: (a) a partially bonded device and (b) a successful bonded component.

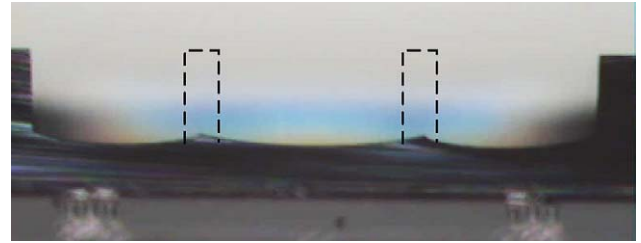


Fig. 5. Silicon structure in cross section, the fixture is etched off.

due to uneven etch rate over the wafer, see Fig. 5. This problem can be solved by using a material etch stop leading to a better control of the dimension of the spring. A thin wafer should also decrease the aspect ratio giving this process step a higher margin. Therefore, an altered process with thin SOI wafers was used as described below.

3.2. SOI fabrication

The SOI processing is similar to the previous described one. A new mask to descend the fixture and the sensitive part of the sensor was designed and the aluminium electrode was stretched out to the edge to prohibit also any bonding of the springs. The fixture is descended to insure that the moveable part is not pulled off during dicing and to reduce the risk of damage during general handling.

Starting material is SOI wafer, 400 μm thick, with a device layer of 13 μm . The buried oxide is 0.6 μm . A recess of 20 μm is etched to lower the whole middle part. Oxide was grown on the wafer, to prepare for the DRIE-etch and the wafer was p++ doped on the backside, see Fig. 6(a). Using double-sided lithography the backside was patterned and etched down to the buried oxide layer, see Fig. 6(b). The grown oxide on the front side was then patterned and the structured was etched to form the fixture and release the springs, see Fig. 6(c). After

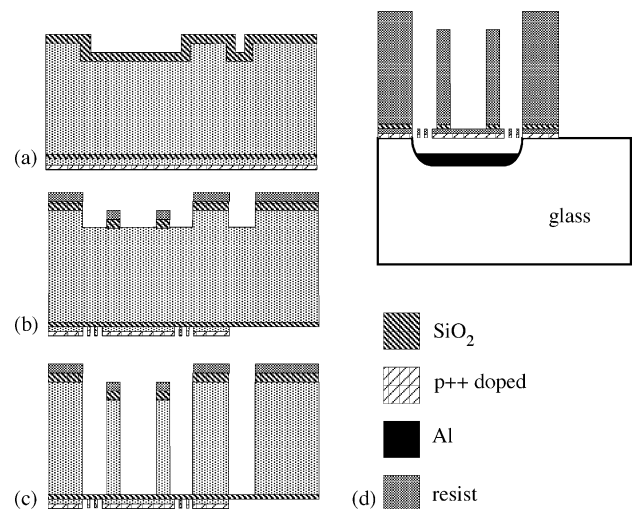


Fig. 6. Schematic of main fabrication step for the SOI fabrication: (a) etched recess and p++ doping, (b) etch of back side to form springs and oxide pattern, (c) deep dry etch and (d) anodic bonding of the structure.

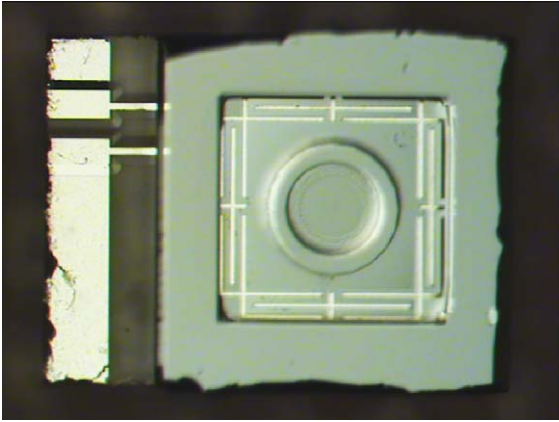


Fig. 7. The manufactured force sensor.

the buried oxide is removed the silicon structure was anodically bonded to a glass substrate process as earlier described, see Fig. 6(d). Here, anodic bonding was performed using a current limitation of 1 mA, which gave better control of the bonding process. The press contact was evaluated using a GaAl contact to the silicon layer. The contact resistance was measured to 30–40 Ω .

A complete force sensor is shown in Fig. 7. The process was found to be very robust and straightforward; the yield of the improved process was nearly 100%.

4. Characterization of the sensor

To evaluate the sensor three methods were used, application of force with a piezoelectric positioning system, electrostatic evaluation and resonance frequency test using scanning laser Doppler vibrometer. The sensor has also been tested in situ in a TEM to evaluate its ability to work in this environment.

4.1. Deflection measurements

The sensors from the first batch were evaluated using a test board with a piezoelectric positioning system. A copper wire attached to the piezoelectric positioning system is pressed against a gold tip mounted on the silicon plate. The wire is moved against the sensor tip a certain distance while measuring the capacitance change using the read-out chip [11]. The test was conducted over a range of 500–1000 nm (Fig. 8). A similar test was done in situ in a TEM. The sensor worked well proving that the sensor operates in the intended environment.

4.2. Spring constant measurements using electrostatic forces

An electrostatic evaluation was done to determine the spring constant of the manufactured structure. A dc-voltage

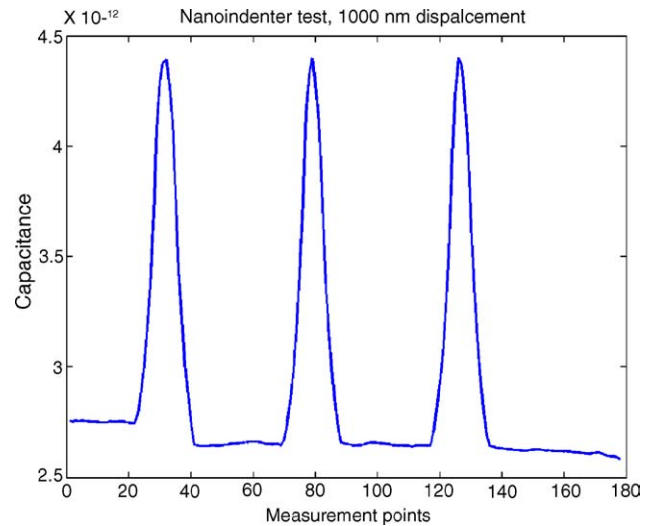


Fig. 8. Measured capacitance while the sensor is pressed 1000 nm in and out, axis show capacitance in pF vs. measured points.

was applied to the sensor while the capacitance was measured. The intention was to measure the snap-in voltage of the sensor, and from that result get the force constant. Snap-in occurs when the gradient of the electrostatic force exceeds the gradient of the spring force. This occurs when the distance is 2/3 of the electrode gap, if the forces are according to Equation (1):

$$F_{\text{electrostatic}} = F_{\text{mechanical}} \Leftrightarrow \frac{\varepsilon \cdot A \cdot V^2}{2 \cdot (d_o - \Delta d)^2} = k \cdot \Delta d \quad (1)$$

where ε is permittivity in air, A the plate area, V the voltage, d_o the electrode distance, Δd is the change in distance of the electrode plates and k is the spring constant. To measure the snap-in event, the voltage was increased until the capacitance of the sensor changed drastically. The snap-in voltage was measured to 12.2 V. All of the parameters were now known, and with $\Delta d_{\text{snap-in}} = d_o/3$ gave a spring constant of 928 N/m.

4.3. Resonance frequency measurements

To characterize the sensor further, resonance frequency measurements were done using a scanning laser Doppler vibrometer a Polytech PSV 300, which scans a surface and measures the velocity at several points. The maximum resolution of the system is 0.3 $\mu\text{m/s}$, which corresponds to a displacement resolution of 50 pm at 1 kHz. Maximum bandwidth of the instrument is 1 MHz. Measurements can be performed in vacuum chamber by measuring through a transparent lid [12].

The experiment was conducted inside a vacuum chamber at 1.2×10^{-4} mbar. An electrical excitation signal was applied to the sensor and the displacement was measured with a laser beam. The frequency was swept from 0 to 20 kHz. The frequency response and the phase are seen in Fig. 9, showing a resonance frequency of 6.6 kHz. The measurement shows

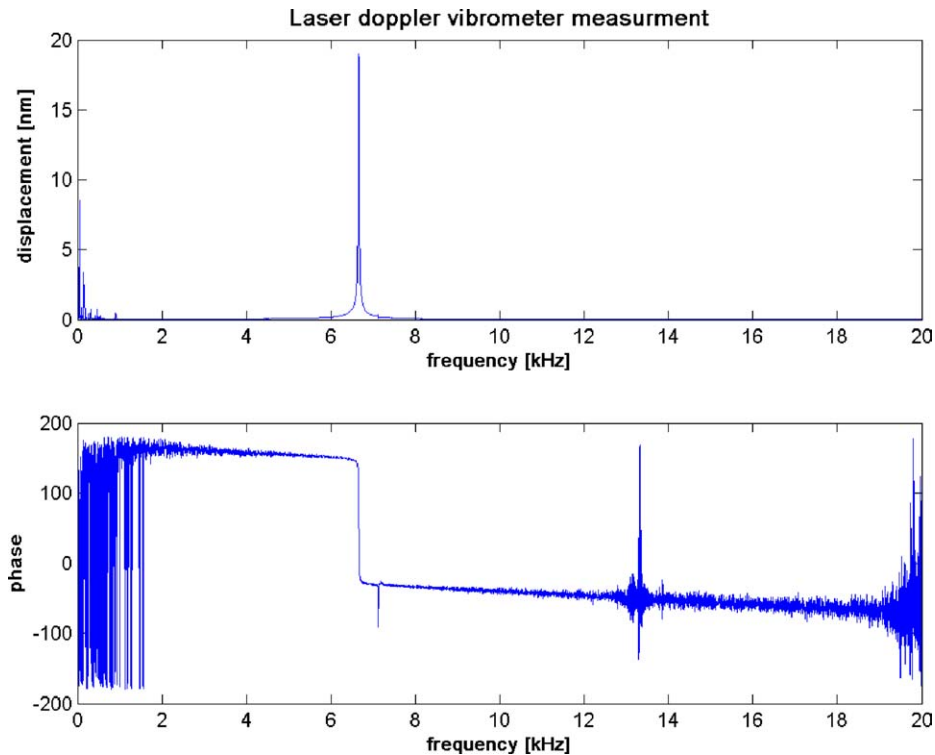


Fig. 9. Frequency and phase response from the scanning laser vibrometer measurements.

a stable fundamental mode with no mode interference. From the same data the Q -value was measured to 440. The spring constant was calculated using the measured resonance frequency and a calculated mass (from the designed geometry of the structure and the density) giving a result of to 750 N/m.

This spring constant value gives a sensitivity of 0.27 fF/0.1 μ N for small deflections. A similar sensitivity of 0.19 fF/0.1 μ N for small deflections is obtained by the electrostatic method. Using existing electronics, this sensitivity is easily measured showing that the sensor fulfils the requirements. However, the difference in sensitivity needs to be investigated further for full characterization.

5. Conclusions

A highly sensitive capacitive force sensor with an integrated fixture for interchangeable tips has been designed and manufactured for in situ nanoindentation applications inside a TEM. The integrated fixture enables a large freedom in the choice of tip materials, e.g. diamond, sapphire etc. Final size of the sensor without tip is 2 mm \times 1.5 mm \times 0.9 mm, which allows a relatively easy mounting in the TEM specimen holder. Three different methods were used to evaluate the force sensor, deflection measurements, electrostatic force measurement and resonance frequency measurement. The sensitivity for small deflections is 0.27 and 0.19 fF/0.1 μ N for resonance frequency and electrostatic methods, respectively. The evaluation shows that the sensor fulfils the requirements

for its application; it operates in a TEM, it yields a sensitivity that is measurable in the 0–100 μ N range and the improved fabrication process has a near 100% yield.

References

- [1] X. Li, B. Bhushan, A review of nanoindentation continuous stiffness measurement technique and its application, *Mater. Charact.* 48 (2002) 11–36.
- [2] M.A. Wall, U. Dahmen, An in situ nanoindentation specimen holder for a high voltage transmission electron microscope, *Microsc. Res. Tech.* 42 (1998) 248–254.
- [3] E.A. Stach, T. Freeman, A.M. Minor, D.K. Owen, J. Cumings, M.A. Wall, T. Chraska, R. Hull, J.W. Morris Jr., A. Zettl, U. Dahmen, Development of a nanoindenter for in situ transmission electron microscopy, *Microsc. Microanal.* 7 (2001) 507–517.
- [4] A.M. Minor, J.W. Morris, E.A. Stach, Quantitative in situ nanoindentation in an electron microscope, *Appl. Phys. Lett.* 79 (2001) 1625–1627.
- [5] A.M. Minor, E.T. Lilleodden, E.A. Stach, J.W. Morris Jr., Direct observations of incipient plasticity during nanoindentation of Al, *J. Mater. Res.* 19 (2003) 178–182.
- [6] A.M. Minor, E.T. Lilleodden, M. Jin, E.A. Stach, D.C. Chrzan, J.W. Morris Jr., Room temperature dislocation plasticity in silicon, *Philos. Mag.* 85 (2005) 323–330.
- [7] Z. Shan, E.A. Stach, J.M.K. Wiezorek, J.A. Knapp, D.M. Follstaedt, S.X. Ma, Grain boundary-mediated plasticity in nanocrystalline nickel, *Science* 305 (2004) 654–657.
- [8] K. Svensson, Y. Jompol, H. Olin, E. Olsson, A compact design of a TEM–STM holder with 3-dimensional coarse motion, *Rev. Sci. Instrum.* 74 (2003) 4945–4947.
- [9] <http://www.nanofactory.com/>.
- [10] www.microsensors.com, MS3110.

- [11] <http://www.smartec.nl>.
- [12] H. Rödjegård, G. Andersson, Characterization of mechanical sensors using multiple pieces of equipment, in: Proceedings of Micro Structure Workshop, Ystad, Sweden, March 30–31, 2004, pp. 93–96.

Biographies

Alexandra Nafari received her masters of science in electrical engineering at Chalmers University of Technology. She is currently sharing her time between PhD studies at Solid State Electronics Laboratory at Chalmers University of Technology and product development at Nanofactory Instruments AB.

Peter Enoksson was born in Lindsberg, Sweden, 1957. He received the MSc degree in engineering physics in 1986, the licentiate of engineering in 1995 and the PhD in 1997 all from the Royal Institute of Technology, Stockholm, Sweden. In 1997, he was appointed assistant professor and in 2000, associate professor at the Silicon Sensor Research Group at the Department of Signals, Sensors and Systems at the Royal Institute of Technology. In 2001, Dr. Enoksson was appointed professor at Chalmers University of Technology where he heads the Microsystems Group. In

2002, he was appointed vice dean of School of Electrical Engineering and in 2003 also head of the Solid State Electronics Laboratory. His research is in the field microsystems and nanosystems, e.g. of resonant silicon sensors and actuators, especially for fluid applications.

Håkan Olin was born in Södertälje, Sweden in 1957. He received his PhD in physics at Chalmers University of Technology in 1993 and was appointed assistant professor in 1994 and associate professor in 1999. In 2003, Dr. Olin was appointed professor in material physics at Mid Sweden University. His research is the field of nanotechnology using scanning probe microscopy and nanofabrication methods.

Andrey Danilov received his PhD in physics at Chalmers University of Technology in 2002. Today, he is sharing his time between product development at Nanofactory Instruments AB and Chalmers, where he was appointed assistant professor in 2003.

Henrik Rödjegård received the master of science degree in electrical engineering in 1997 from Chalmers University of Technology, Göteborg, Sweden. Presently, he is a graduate student in the Mechanical Sensor Group at the IMEGO Institute in Göteborg. His research focuses on bulk micromachining and design of sensor electronics.